JJMIE

Volume 18, Number 3, September. 2024
ISSN 1995-6665
Pages 461- 470
https://doi.org/10.59038/jjmie/180302
Editor-in-Chief: Prof. Ali M. Jawarneh

Jordan Journal of Mechanical and Industrial Engineering

Surface Improvement of Titanium Alloys for Biomedical Applications by Anodizing

Eman Yasir Hussein*, Jassim M. Salman Al-Murshdy, Nabaa Sattar Radhi

Metallurgical Engineering Department/College of Materials, Engineering/University of Babylon, Iraq

Received 21 Jan 2024 *Accepted 19 May 2024*

Abstract

The electrochemical oxidation experiment utilized an electrolyte solution of 0.8M NaF in 1M H_3PO_4. An applied voltage of 10 V was utilized, and the experiment was carried out for three different time durations: 15, 30, and 45 minutes. Hence, this study aims to explore the impact of anodic oxidation of titanium alloy under specified conditions on the structural and morphological characteristics, wettability features, and electrochemical behavior of both the untreated surface and the surface modified by the development of titania (TiO_2) layers. Following the anodization procedure, the samples underwent analysis utilizing several characterization techniques. The anodized samples' surface morphology was analyzed using various techniques, including SEM, EDS, XRD, contact angle measurements, AFM, electrochemical measurements (corrosion rate), and pH measurements of the solution. The best sample, B, was obtained. Titanium oxide has the highest corrosion resistance, the appearance of the titania phases, and is hydrophilic, thus having the most compatibility.

Keywords: Anodizing, Titanium alloys, electrochemical, TiO_2, Voltage, Time.

1. Introduction

Anodization is a chemical procedure that thickens and stabilizes the oxide deposit on some metals and alloys [1]–[6].The color of electrochemically oxidized titanium is interference coloring, which is controlled by the difference in potential applied and is a function of the oxide layer's thickness formed [7]–[12]. The oxide's thickness varies between a few nanometers and a few micrometers, and the colors produced are vibrant and different. Titanium, platinum, stainless steel, nickel, lead, or Carbon as a conductor to the electrochemical solution to the negative pole (cathode) [13]–[15].Upon the closure of the circuit, the anode metal undergoes electron extraction, while the cathode facilitates the return of electrons to the electrolytic solution. Subsequently, these electrons react with the hydrogen present in the water, generating molecular hydrogen. The metal cations at the anode undergo a reaction with water, forming an oxide layer on the surface of the metal [16], [17]. The initial stage of titanium anodic oxidation involves the creation of an oxygen-enriched layer on the surface of the metal, specifically on the pre-existing "natural" oxide film [18]. To initiate the oxidation process, oxidizable species must exist within the system. The anticipated impact on development is equivalent to transferring Ti2+ and O2- ions onto the pre-existing oxide layer. Irrespective of the current density, researchers assume a linear correlation exists between the formed oxide layer's thickness and the applied ultimate potential [19]. The oxide is currently hypothesized to be TiO2, exhibiting a surplus of titanium atoms near the oxide-metal interface, while an excess of oxygen atoms is observed at the oxide-solution interface to promote the migration of metal atoms. In a general context, the process of anodic oxidation typically yields the formation of the anatase structure. However, when anodic oxidation is subsequently followed by heat treatment, it is found in the formation of the rutile structure [20]–[22].

The oxide layer's surface morphology and magnitude are dictated by the methodology employed in fabricating the oxide coating. The morphology and the oxide film's thickness are crucial in determining the implant's response to the surrounding environment. The chromaticity of the oxide generated through anodic oxidation may approximate the magnitude of the coating's thickness. The color and thickness of the oxide are significantly impacted by the anodization procedure and the electrolyte's composition [23]. Any deviation in these parameters has the potential to modify the hue of the titanium oxide coating. While investigating surface oxide preparation, it was observed that the electrochemical growth characteristics of the oxide film on titanium (Ti) metal exhibit a significant reliance on various anodic parameters. These parameters include agitation speed, temp, anodic forming voltage, applied current density, electrolyte amount, and the ratio of the cathode to anode surface areas [24]–[28]. One of the biggest obstacles to implant-prosthetic medicine is connective tissue reintegration [6], [29]. The barrier between the soft tissues and the surface of the trans-mucosal component has

* Corresponding author e-mail: hsynaymanyasr@gmail.com.

received greater attention lately. It is now thought that the most important thing to protecting the implant from infection by bacteria and lowering the risk of peri-implant is stabilizing the connection between the connective tissue and the epithelial attachment on the abutment surface (in the case of a bone-level implant or on the implant neck (in the case of a tissue-level implant). However, improving the implant survival rate has been the main focus of attention over the past ten years of osteointegration [30].

Additional methods, like biomechanical alterations, have been suggested to increase the surface biological function of Ti substrates.(micro-grooving, chemical etching, and abrasion)Three types of modification: biological, psychological, and physical (laser, collagen, hydroxyapatite, nanoparticles). Nano-engineered surfaces have attracted attention among these alterations due to their resemblance to these extracellular matrix substrates. Although several techniques have been reported to produce a nanotextured surface, electrochemical oxidation, also known as anodized oxidization, has been considered the most widely utilized and economical method for creating a nano-structured TiO_2 oxide film [31]. Itzel et al. investigated the anodic oxidation using an approach to generate nanotubes with a constant work potential of 60 V but with varying anodizing periods of (10, 20, 30, 40, 50, and 60) min to investigate their impact on nanotube features and biological activity [32]. Ossowska et al. [33] investigate the impact of two-stage anodization (in phosphoric acid for 30 minutes) in the occurrence of hydrofluoric acid in the second step [34]. Al-Lestari1a et al. research Surface modification of TiO_2 layer development which is commonly utilized to increase biological, chemical, and mechanical features.

Electrochemical anodization of Ti-6Al-4V in an H_3PO_4+NH_4F solution yields TiO_2 nanostructures under self-organization conditions. Najim et al. investigated the anodization of a commercial pure titanium (CP-Ti) substrate in an electrolyte containing 0.8M NaF in 1M H_3PO_4 at a constant applied voltage of 10 V for (30, 90, and 150) minutes [25], [35]. Agnieszka et al. [36] investigated the impact of anodizing treatments on the micromechanical and biotribological features of the Ti-13Zr-13Nb alloy. Anodizing was utilized to create 1st-generation, 2nd-generation, and 3rd-generation (1G, 2G, and 3G) ONT layers on the Ti-13Zr-13Nb alloy surface. Jak. et al. [37], examined the biofunctionalization of the titanium surface utilizing electrochemical anodic oxidation. It was discovered that the Ti surface is primarily covered by anatase-TiO_2 after anodic oxidation in an electrolyte comprised of H_3PO_4 and HF.

The anodizing method was utilized in this work as a promising approach to improve significantly the surface structure and features of Ti 13Nb 13Zr alloy. Depending on the kind of substance, the following variables can influence the anodizing process such (time, electrolyte, voltage)Using 10 volts and forming a stable oxide layer, using phosphoric acid at a distance of 3 cm.

2. Materials and Methods

In this study, Ti alloy specimens were utilized as the primary substrates for the anodization procedure to generate TiO_2. Table 1. Chemical analysis was done using an X-ray fluorescence (XRF) test at Baghdad, Iraq's Ministry of Science and Technology.

The Ti alloy samples underwent an initial grinding process utilizing silicon carbide abrasive sheets with grit sizes ranging from 180 to 1000. It is commonly used to remove material from the workpiece, to produce a smooth finish on the surface of the workpiece, or to remove burrs from the surface, and it has sufficient surface properties.

Subsequently, the samples were subjected to successive ultrasonic cleaning in acetone and distilled water for 10 minutes each. Finally, the samples were dried using hot air. An anodic oxidation method was employed to modify the surface of titanium samples, which was achieved by utilizing a typical two-electrode configuration with stirring at ambient temperature.

The experimental setup involved the utilization of a Ti13Nb13Zr alloy specimen and a 316L stainless steel (13Ø,3mm thickness) as the anode and cathode, respectively. The two electrodes were meticulously positioned in direct contact with the cell's electrolyte. In all experimental trials, the separation distance between the two electrodes was maintained at a constant value of 3 cm.

The anodic oxidation process was conducted in a glass beaker, with magnetic stirring to maintain the dispersion of the homogenous particles throughout, as depicted in Fig. 1. The system is fitted with a direct current (DC) power source operating at a potential of 10 volts, with periods of 15, 30, and 45 minutes. For every experiment, 100 ml of electrolyte was prepared.

The electrolyte solution was prepared as follows:

1. 1M of H_3PO_4

The density of 98% phosphoric acid =1.83 g/ml, The molecular weight of H3PO4 = 98 g/mol**.**

$$M_{H3PO4}=\frac{\%\text{ age H3PO4}\times\rho\times1000}{\text{Mole.wt of H3PO4}}=\frac{1\times1.83\times1000}{98}=18.67$$

$$M1\times V1=M2\times V2\rightarrow V1=\frac{1\times50}{18.67}=2.67\text{ml}$$

2. 0.8M of NaF

The molecular weight of NaF = 41.988 g/mol.

$$wt.\%=\frac{M\times\text{Mole.Wtof NaF}\times V}{1000}=\frac{0.8\times41.988\times50}{1000}=1.67\text{g}$$

Thus, 1.67g of NaF was added to 48.33 ml of distilled water(DH2O), mixing by stirring until it melted, and 2.67 ml of H3PO4 was added to 47.33 ml of DH2O. Thus, according to relevant empirical calculations, we obtained the electrolyte solution of 100 ml. Afterward, this prepared electrolyte was stored in a clean 120 ml beaker for the subsequent anodization. Proper safety measures were taken during handling the electrolyte.

Table 1. Chemical composition of the Ti-13Nb-13Zr alloy (wt.%)

Elements	Zr	Nb	Fe	Mo	Zn	Mn	Cu	Ti	Residual Element
Concentration (%)	15.22	13.45	0.1155	0.077	0.0527	0.0387	0.0432	Balance	0.13505

3. Test Results and Discussion

3.1. Light Optical Microscope (LOM)

The optical microscope technique was employed to examine the microscopic structure to identify the present phases and observe the morphology and dimensions of the grains. This analysis was conducted after the grinding and polishing processes, followed by etching in a solution (swab) with a base, as depicted in Figure 2. The titanium alloy Ti 13Nb 13Zr, sometimes known as a two-phase alloy, is being discussed. The composition primarily comprises a single phase (β) and a single phase (α), along with a microstructure [34], subsequent to the process of Anodizing, as illustrated in Figure 3. The microscope in question belongs to the BEL PHOTONICS type.

A TiO_2 layer and uniform coating findings can be observed on the surfaces of the specimens that underwent anodization for 15 and 30 minutes, as depicted in Figure 3(A, B). As depicted in Figure 3 (C), the microstructure exhibits a limited number of black cracks after 45 minutes.

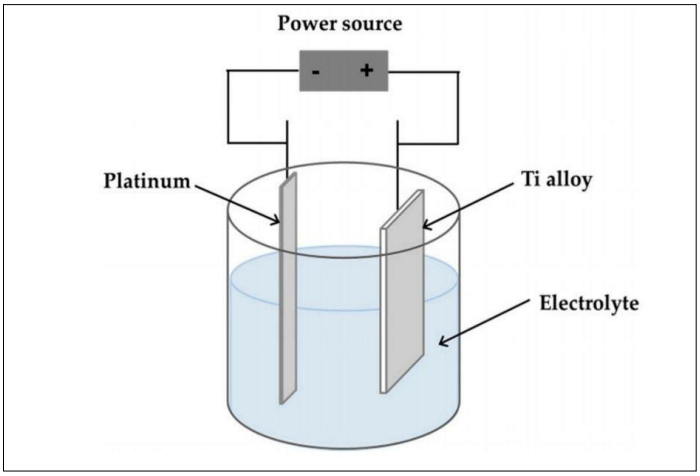

Figure 1. Schematic Illustration of the Anodization Equipment[38].

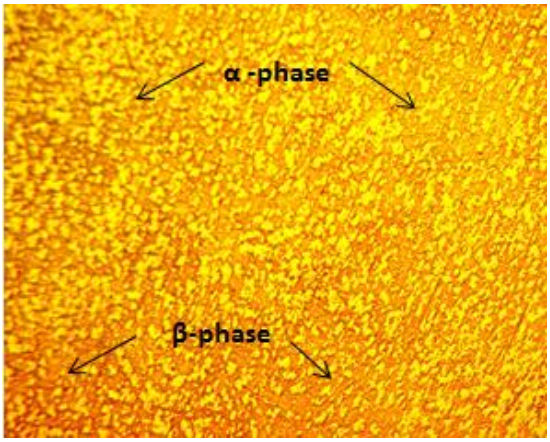

Figure 2. Microstructure of the Ti alloy after etching with the Kroll solution(swab) composed of 10 HF+ 5 HNO_3 + 85 H_2O by utilizing microscope magnification (400X).

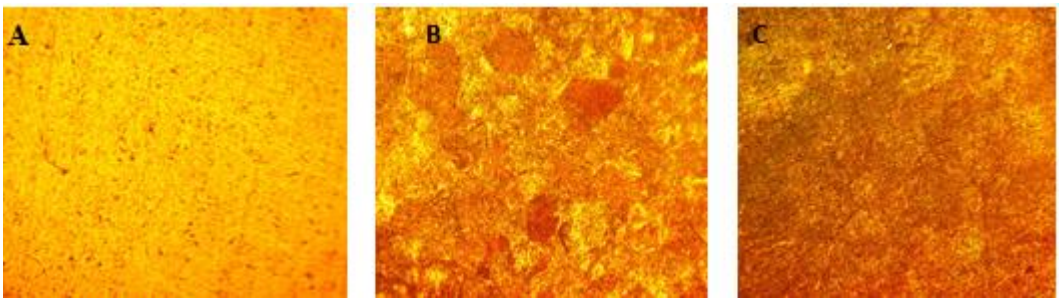

Figure 3. Optical microscope images of the film were deposited after anodization (100X) at 10V for (A) 15 minutes, (B) 30 minutes, and (C) 45 minutes A anodization process.

3.2. Scan Electrons Microscopy Analysis

The scan electron microscope type (VEGA3SBU) was used to assess the surface morphology of Ti-Nb-Zr alloy substrates. An energy-dispersive X-ray spectrometer (EDS) was utilized to detect the distribution of elements in the oxide layer.

Scanning electron microscopy (SEM) pictures depicting the surface morphology of the TiO_2 layer on the titanium alloy following anodization for 15 and 30 minutes in the presence of a uniform coating are presented in Figures 4 A and B, respectively. Additionally, surface fissures (Figure 4 C) were discovered on the TiO_2 coating, visible on its surface. These cracks can be linked to the prolonged exposure of the coating's surface for 45 minutes, recognized as one of the primary factors contributing to crack formation. The protective layer film is the initial layer of film that forms on the titanium surface after anodization. Due to its thick and insulated structure, this film is known as a barrier film. Usually, this is extremely thin. Its thin form makes it extremely limited in application. It is locally essential to supply the process of cracking barrier film, which has insulating qualities, to enhance its thickness.

Previous studies have demonstrated that electrochemical process variables, including ion current density, solution, temperature, and voltage that are used, influence the characteristics of the titanium oxide coatings created during anodizing, figure 4 take in magnification power 3000x.

However, applying too low potentials often results in the growth of the anodic films with completely clogged pores, in addition, a special emphasis is put on the generation of the internal cracks and fractures within the anodic films. It should be mentioned that many research groups have reported O2 evolution as a significant factor in the generation of pores and voids in anodic films during anodization of various metals, e.g., Ti. In addition, a special emphasis is put on the generation of the internal cracks and fractures within the anodic films [39].

Figure 5 depicts the Energy Dispersive Spectroscopy (EDS) study of the surfaces of Ti-13Nb13Zr that have undergone modification by the anodizing process, specifically at a voltage of 10 V for a duration of 30 minutes(best result). The findings validate the existence of a Ti oxide layer in the sample, which can be attributed to the elevated concentrations of Titanium (Ti) and Oxygen (O) elements, the primary constituents of TiO_2. Trace amounts of nitrogen (N) and zirconium (Zr) can also be observed on the anodized surface.

3.3. X-Ray Diffraction

The diffraction pattern shown in Figure 6 exhibited the presence of both beta and alpha phases, which corresponded to the JCPDS Card No. (044 - 1294). The composition of the Ti-13Nb-13Zr alloy mainly comprises β-Ti and α-Ti,Agree and Agnieszka et al [80] It can be seen that the Ti-13Nb-13Zr alloy mainly consists of β -Ti and α –Ti**.** is predominantly composed of β-Ti and α-Ti. The X-ray diffraction (XRD) data are shown. This study confirms the production of TiO2 layers exhibiting a comparable crystalline phase on the surface of a titanium alloy following treatment. An anodization process was performed on the optimal specimen at a voltage of 10V for 30 minutes(best sample). The presence of newly generated TiO2 peaks upon anodization may be observed, as depicted in Figure 7, which corresponds to the ICSD card No. (017009).

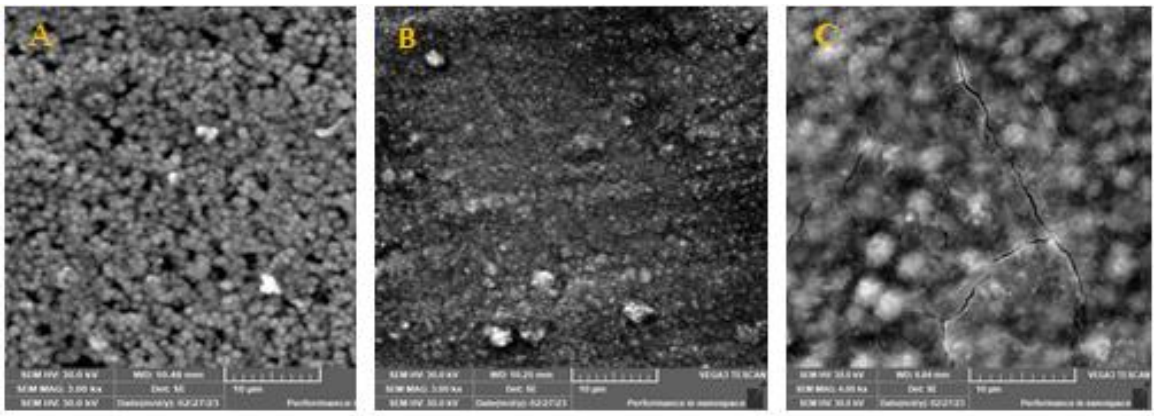

Figure 4. The titanium oxide layer on the Ti alloy surface was 10V for (A) 15 minutes, (B) 30 minutes, and (C) 45 minutes of anodization.

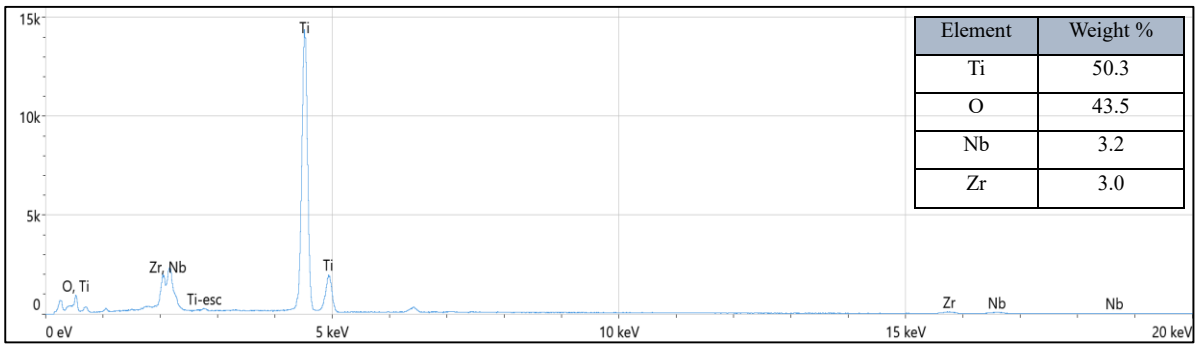

Element	Weight %
Ti	50.3
O	43.5
Nb	3.2
Zr	3.0

Figure 5. EDS examination of B specimen.

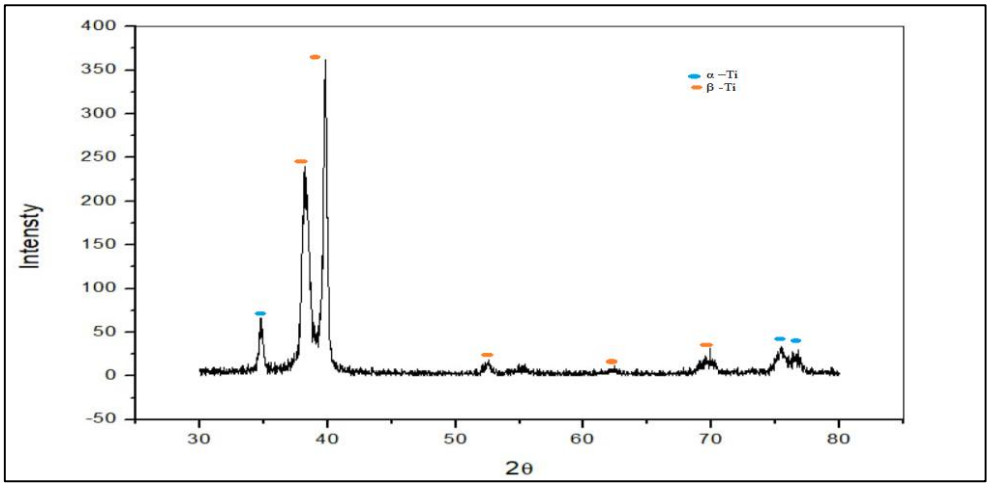

Figure 6. XRD Pattern of Ti–13Nb–13Zr Alloy

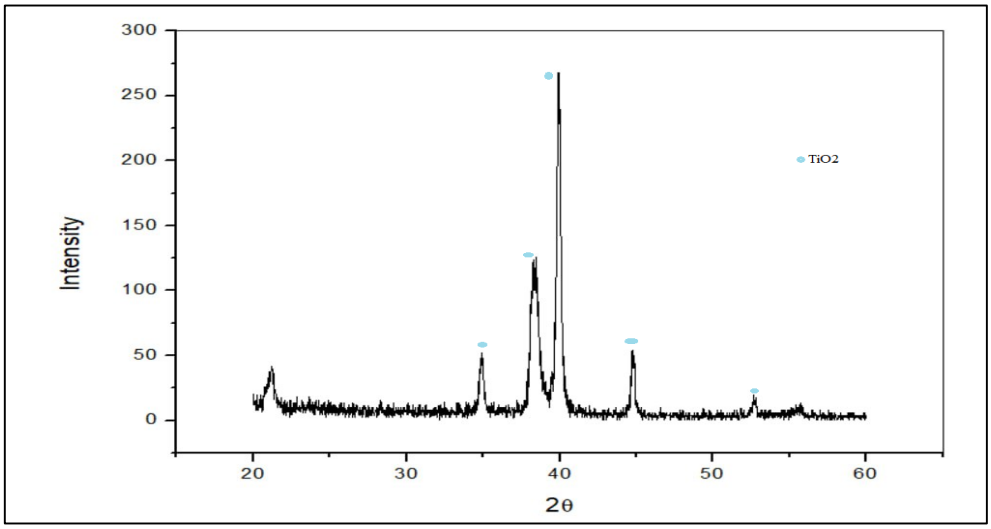

Figure 7. XRD profiles of the anodized sample (B) at (10 volts, 30min)

3.4. Atomic Force Microscopy (AFM)

Atomic Force Microscopy (AFM) is a widely recognized and extensively employed technology for the purpose of topographical mapping and investigation of material features at the nanoscale. The surface topography of the examined TiO_2 layer, comprising three-dimensional (2D,3D) pictures and layer thickness, was detected utilizing an AFM model Nano AFM 2022 manufactured by Nano Surf in Switzerland.

The findings strongly concur with the average roughness characteristic of the AFM examination. Multiple studies have demonstrated that surface roughness within the range of 1 to 10 µm enhances the level of contact between the bone and the implant's surface. According to a study conducted by researchers [40], it has been observed that titanium surfaces that are smoother in texture exhibit less effective interaction with bone tissue in comparison to rougher surfaces. The surface roughness should be appropriate to facilitate the process of osteointegration between titanium (Ti) and the surrounding tissue. The AFM test findings for the Ti-13Nb-13Zr alloy, as listed in Table 2, indicate a core roughness depth (Sa) of 68.43 nm. These findings align with the 3D images obtained from the Atomic Force Microscopy (AFM) test, as depicted in Figure 8.

AFM is employed to quantify the thickness of a coating on a 13Nb 13Zr alloy. The deposition of titanium dioxide (TiO_2) by the process of anodization is conducted in this study. Similarly, the Atomic Force Microscopy (AFM) analysis demonstrated that the observed film thickness of the B sample was determined to be 311.5nm, as illustrated in Figure 9)a. These findings indicate that the proposed methodology is appropriate for measuring thin film thickness.Thickness values were estimated by lateral view SEM images. Figure (9)b presents the cross-section view of the anodic oxide layer formed on the sample (30 min).

Table 2. S q, S z, Sa AFM features of TiO_2 layer.

ISO- 25178-Primary Surface	
Sq (Root-mean-square height)	83.54 nm
Sz (Maximum height)	503.7 nm
Sa (Arithmetic mean height)	68.43 nm

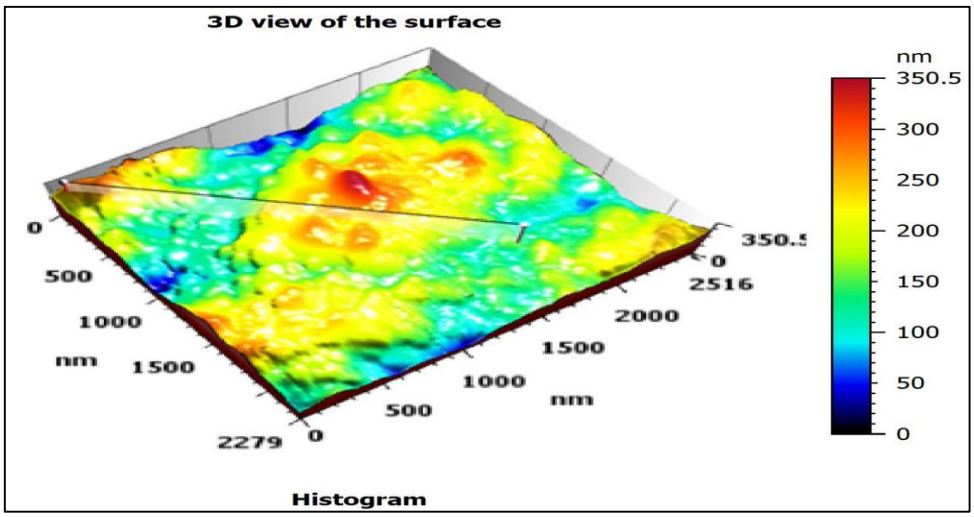

Figure 8. AFM 3D profiles for the anodization process of sample B.

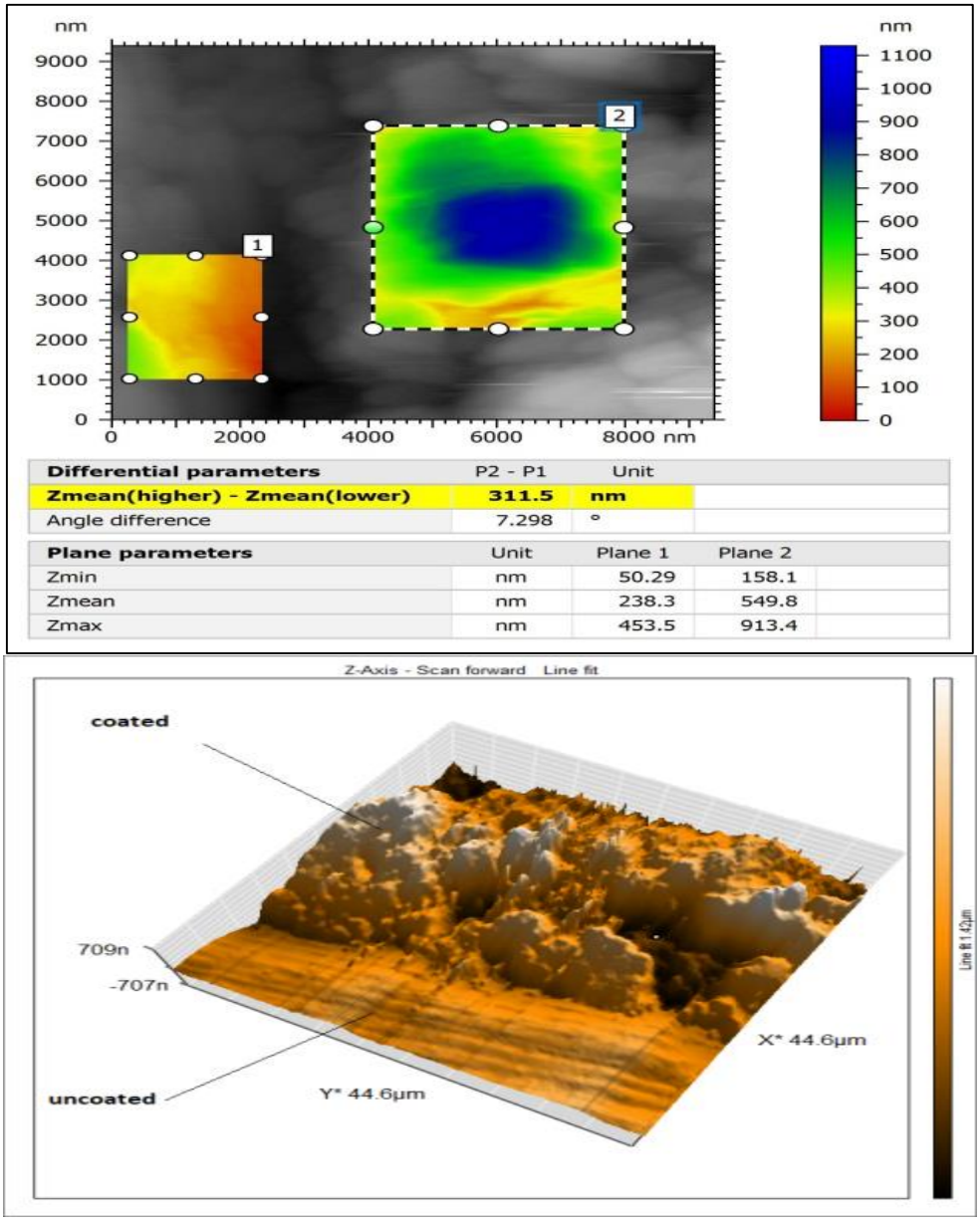

Differential parameters	P2 - P1	Unit
Zmean(higher) - Zmean(lower)	311.5	nm
Angle difference	7.298	°

Plane parameters	Unit	Plane 1	Plane 2
Zmin	nm	50.29	158.1
Zmean	nm	238.3	549.8
Zmax	nm	453.5	913.4

Figure 9. a. AFM 3D profiles for thin film thickness TiO_2 after anodization process of B sample.

3.5. Contact Angle Test

The contact angle is commonly utilized to determine a surface's wettability. The hydrophobicity or wet ability of anodized Ti 13Nb 3Zr alloy and unanodized samples were assessed utilizing the static contact angle (θ) of a droplet on a solid surface, which is an essential index for quantitatively evaluating solid surface wettability.

Once a droplet of liquid meets a surface, it gives rise to a contact angle, which is determined by the interplay between the liquid's surface tension and the surface's free energy. The angular measurement characterizes the interfacial interaction between the liquid substance and the contacting surface. In materials engineering, when the contact angle surpasses 90°, it is conventionally inferred that the surface is deemed dry. Once the contact angle is below 90°, the morphology of the liquid droplet interacting with the substrate transforms. In this scenario, it is necessary to ascertain the time-dependent contact angle dynamically. A liquid droplet deposited onto a solid substrate with non-absorbent features undergoes a progressive process towards attaining a state of equilibrium. The contact angle readout yields the numerical value of the static contact angle. Table 3 Optical images of contact angles after 15sec of samples after anodizing. The contact angles of the substrate were measured to be 67.367º, and the anodized samples treated at 10V for A(15min) and B(30min) were measured to be 33.792º,30.203º respectively. This study of TiO_2 generated by the Anodization of Ti can improve the hydrophilicity without changing the morphology. Furthermore, it was found that the increased wettability of the surface Ti alloy sample is essential for promoting osteogenic cell adhesion and differentiation [41].

The findings of this study indicate that the synthesized TiO_2 exhibits an enhanced hydrophilic characteristic, which can be further optimized through meticulous parameter selection. Consequently, manipulating anodization parameters presents a promising approach for modifying surface features. The correlation between enhanced surface hydrophilicity and the degree of protein and cellular adhesion has been established through multiple studies, which, in turn, can have a notable influence on the proliferation and differentiation of cells. Consequently, employing this technique can serve as an effective means of enhancing the biocompatibility of metallic implant surfaces [42].

3.6. Electrochemical Corrosion

In this study, the corrosion behavior of Ti 13Nb 13Zr was examined both prior to and after the experimental procedures. Anodizing was achieved using an electrochemical cell of three electrodes [43], [44]. Polarization tests were conducted utilizing a potentiate known as the "Winking M Lab 200." The potentiodynamic polarization curves were plotted. Tafel plots were employed to measure the corrosion potential (Ecorr.) and corrosion current density (Icorr.) utilizing both anodic and cathodic polarization branches, as presented in Table 4. The studies were conducted under ambient conditions, specifically at room temperature, utilizing a solution of 0.9% sodium chloride (NaCl), commonly referred to as "Normal Saline," as depicted in Figure 10.

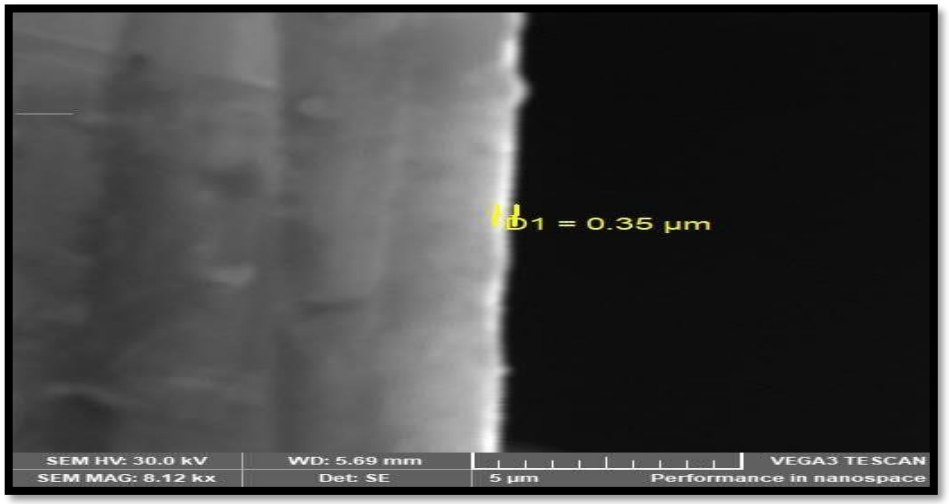

Figure 9. b: Cross-section SEM images for : (B) TiO_2 layer

Table 3. Contact angle (θ º) of Ti 13Nb 13Zr alloy and anodized samples.

Specimens	Base	A	B
Degrees	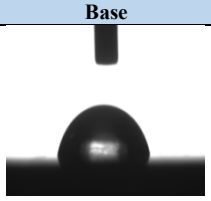 67.367 º	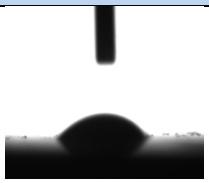 33.792º	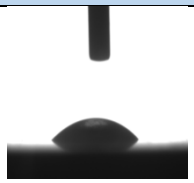 30.203º

3.7. Calculation of the pH of Solution

The pH is a quantitative indicator of the hydrogen ion concentration, which determines the level of acidity or alkalinity in each solution. The pH scale typically ranges from 0 to 14. The pH of the samples was determined utilizing a Hanna HI-8424 Handheld Water Resistance pH Meter both before and after the anodization procedure. Variations in the pH levels of the electrolyte result in distinct current density profiles and surface patterns of TiO_2[45]. The initial pH of the solution before anodization was determined to be 1.71. In other words, a solution with a high concentration of hydrogen ions. Following the anodizing procedure, the solution's acidity experienced a reduction, resulting in a recorded value of 2.41. The observed phenomenon in Figure (11) illustrates the alteration in the solution's color due to the downward movement of ions and the subsequent sedimentation process of the TiO_2 layer.

Table 4. Electrochemical parameters of Ti 13Nb13Zr substrate and A, B Specimens in 0.9NaCl (Normal Saline).

NO.	Sample code	I corr. (µA)	E corr.(mv)	Corrosion Rate (mm/y)
BASE	/	6.26	59.1	0.0190
A	15min	1.21	138.4	0.0036
B	30min	630.50 $\times 10^{-3}$	146.5	0.0213×10^{-3}

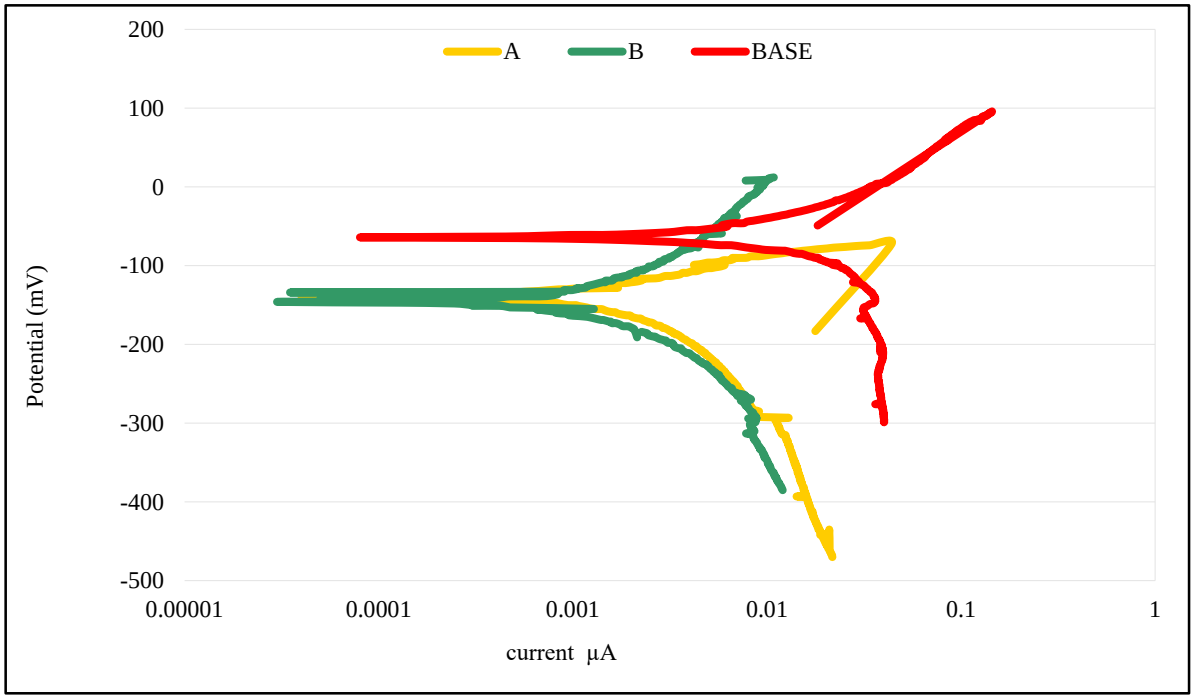

Figure 10. Potentiodynamic polarization curves of base and A, B samples in(0.9NaCl) the Normal Saline solution.

Figure 11. Image of pH Meter and solution anodization.

4. Conclusion

This study aimed to achieve TiO_2 nanostructures on the surface of Ti 13Nb 13Zr alloy substrates utilizing anodizing treatment to explore their potential in biomedical applications. Various factors, including applied voltage and time, were systematically varied to investigate their influence on the resulting nanostructures. The nanostructures have been subjected to characterization in terms of their shape, phase composition, wettability, and corrosion features. The primary findings of this study can be succinctly summarized as follows:

- Adjusting the anodizing parameters, specifically the applied voltage and time can create various morphologies of TiO2 structures. Applying a voltage of 10V for 30 minutes during the anodizing process results in forming a more uniform oxide structure. The anodized specimen was eliminated from consideration after being subjected to a voltage of 10 V for 45 minutes since it exhibited crack formation inside the TiO_2 layer.
- The wettability analysis was employed to investigate the wetting characteristics of the untreated and treated titanium samples. The contact angle of the samples was assessed by using normal saline. Based on the acquired data, it can be shown that the anodized Ti samples exhibited significantly reduced wettability in comparison to the base surface. Among the various oxidized Ti samples, the droplet contact angles were most favorable for the samples subjected to treatment at (10 V, 30 min).
- Among all the Ti-alloy samples examined, the samples subjected to anodization at 10V for 30 minutes exhibited more uniform and superior surface characteristics. The maximum level of corrosion resistance is observed in a 0.9 molar sodium chloride (NaCl) solution.
- In this regard, differences in surface structure regarding surface morphology of TiO_2 oxide layers were demonstrated between Ti samples oxidized at 10V. The specimen showed the most significant level of corrosion resistance. Anodized for 30 min (B). For these anodized conditions, sample B recorded the lowest current density (i corr.= 630n A /cm^2) compared to that of the other anodized samples
- Anodizing treatment is often imperative to enhance the corrosion resistance of titanium alloy. The X-ray diffraction (XRD) analysis substantiated the prevalence of TiO2 on the surface under investigation.
- This alloy satisfies the criteria for materials utilized in medical implants. The Ti-13Nb-13Zr alloy has demonstrated efficacy in bone implants.

References

[1] E. Mohammed and Z. Al-khafaji, "Effect of Surface Treatments by Ultrasonic on NiTi Biomaterials," *ACADEMIC JOURNAL OF MANUFACTURING ENGINEERING*, vol. 21, no. 3, pp. 1–6, 2023.

[2] R. Das, M. K. Pradhan, and C. Das, "Prediction of surface roughness in Electrical Discharge Machining of SKD 11 TOOL steel using Recurrent Elman Networks," *Jordan Journal of Mechanical and Industrial Engineering*, vol. 7, no. 1, 2013.

[3] A. Ismail, R. Zenasni, K. S. M. Amine, and S. Ahmed, "Effect of tempering temperature on the mechanical properties and microstructure of low alloy steel DIN 41Cr4," *Jordan Journal of Mechanical and Industrial Engineering*, vol. 13, no. 1, pp. 9–14, 2019.

[4] S. Dwivedi and S. Sharma, "Optimization of Resistance Spot Welding Process Parameters on Shear Tensile Strength of SAE 1010 steel sheets Joint using Box-Behnken Design.," *Jordan Journal of Mechanical and Industrial Engineering*, vol. 10, no. 2, 2016.

[5] Y. Liu, L. He, and S. Yuan, "Wear Properties of Aluminum Alloy 211z. 1 Drilling Tool.," *Jordan Journal of Mechanical and Industrial Engineering*, vol. 15, no. 1, 2021.

[6] Z. S. Al-khafaji, N. S. Radhi, and S. A. Mohson, "Preparation and modelling of composite materials (polyester-alumina) as implant in human body," *International Journal of Mechanical Engineering and Technology*, vol. 9, no. 4, pp. 468–478, 2018.

[7] I. A. U. Kadhim, H. A. Sallal, and Z. S. Al-Khafaji, "A Review in Investigation of Marine Biopolymer (Chitosan) for Bioapplications," *ES Materials & Manufacturing*, vol. 21, 2023, doi: 10.30919/esmm5f828.

[8] A. R. I. Kheder, N. M. Jubeh, and E. M. Tahah, "Fatigue Properties under Constant Stress/Variable Stress Amplitude and Coaxing Effect of Acicular Ductile Iron and 42 CrMo4 Steel.," *Jordan Journal of Mechanical and Industrial Engineering*, vol. 5, no. 4, 2011.

[9] R. N. Hwayyin and A. S. Ameed, "The Time Dependent Poisson's Ratio of Nonlinear Thermoviscoelastic Behavior of Glass/Polyester Composite.," *Jordan Journal of Mechanical and Industrial Engineering*, vol. 16, no. 4, 2022.

[10] M. D. Al-Tahat and A.-R. Abbas, "Activity-based cost estimation model for foundry systems producing steel castings.," *Jordan Journal of Mechanical and Industrial Engineering*, vol. 6, no. 1, 2012.

[11] M. Hamdan, M. Shehadeh, A. Al Aboushi, A. Hamdan, and E. Abdelhafez, "Photovoltaic Cooling Using Phase Change Material.," *Jordan Journal of Mechanical and Industrial Engineering*, vol. 12, no. 3, 2018.

[12] N. S. Radhia, N. E. Kareemb, Z. S. Al-Khafaji, N. M. Sahig, and M. W. Falah, "Investigation Biological and Mechanical Characteristics of Hybrid PMMA Composite Materials as Prosthesis Complete Denture," 2022.

[13] N. M. Dawood, N. S. Radhi, and Z. S. Al-khafaji, "Investigation Corrosion and Wear Behavior of Nickel-Nano Silicon Carbide on Stainless Steel 316L," vol. 1002, pp. 33–43, 2020, doi: 10.4028/www.scientific.net/MSF.1002.33.

[14] Z. S. Al-khafaji, N. S. Radhi, and S. A. Mohson, "Preparation and modelling of composite materials (polyester-alumina) as implant in human body," *International Journal of Mechanical Engineering and Technology*, vol. 9, no. 4, 2018.

[15] A. H. Haleem, N. S. Radhi, N. T. Jaber, and Z. Al-Khafaji, "Preparation and Exploration of Nano-Multi-Layers on 316l Stainless Steel for Surgical Tools," *Jordan Journal of Mechanical and Industrial Engineering (JJMIE)*, vol. 18, no. 2, 2024.

[16] A. H. Jasim, N. S. Radhi, N. E. Kareem, Z. S. Al-Khafaji, and M. Falah, "Identify and Investigation Corrosion Behavior of Electroless Composite Coating on Steel Substrate," *Open Engineering*, vol. inpress, 2023.

[17] K. M. Abed, N. S. Radhi, A. H. Jasim, Z. S. Al-Khafaji, S. Radhi, and S. A. Hussien, "Study the effect of adding zirconia particles to nickel–phosphorus electroless coatings as product innovation on stainless steel substrate," *Open Engineering*, vol. 12, no. 1, pp. 1038–1045, 2022, doi: 10.1515/eng-2022-0364.

[18] S. Sattar *et al.*, "Corrosion reduction in steam turbine blades using nano-composite coating," *Journal of King Saud University-Science*, vol. 35, no. 8, p. 102861, 2023, doi: 10.1016/j.jksus.2023.102861.

[19] A. Aladjem, "Anodic oxidation of titanium and its alloys," *Journal of Materials Science*, vol. 8, pp. 688–704, 1973.

[20] H. Habazaki, K. Shimizu, S. Nagata, P. Skeldon, G. E. Thompson, and G. C. Wood, "Ionic transport in amorphous anodic titania stabilised by incorporation of silicon species," *Corrosion Science*, vol. 44, no. 5, pp. 1047–1055, 2002.

[21] U. Zada, K. Haleem, M. Saqlain, A. Abbas, and A. U. Khan, "Reutilization of Eggshell Powder for Improvement of Expansive Clayey Soil," *Iranian Journal of Science and Technology, Transactions of Civil Engineering*, vol. 47, no. 2, pp. 1059–1066, 2023.

[22] S. A. Hamza and N. S. Radhi, "Composite Coating Using (Hap-Nano Silver) By Macro Arc Oxidation Procedures Was Used To Study the in-Vivo Properties of Titanium Substrate," *Academic Journal of Manufacturing Engineering*, vol. 21, no. 1, pp. 65–71, 2023.

[23] B.-S. Kang, *On the Bone Tissue Response to Surface Chemistry Modifications of Titanium Implants*. 2011.

[24] J. Speight, *Lange's handbook of chemistry*. McGraw-Hill Education, 2005.

[25] B. Al-Zubaidy, N. S. Radhi, and Z. S. Al-Khafaji, "Study the effect of thermal impact on the modelling of (titanium-titania) functionally graded materials by using finite element analysis," *International Journal of Mechanical Engineering and Technology*, no. 1, 2019.

[26] N. S. Radhi, H. H. Jamal Al-deen, R. Safaa Hadi, nada Al-Ghaban, and Z. S. Al-Khafaji, "Preparation And Investigation A Hydroxyapatite Layer Coating On Titanium Substrate For Surgical Implants.," *Journal of Nanostructures*, 2023, [Online]. Available: https://jns.kashanu.ac.ir/article_113861.html

[27] N. S. Radhi and Z. Al-Khafaji, "Investigation biomedical corrosion of implant alloys in physiological environment," *International Journal of Mechanical and Production Engineering Research and Development*, vol. 8, no. 4, 2018, doi: 10.24247/ijmperdaug201827.

[28] Jasim Ahmed Jasim;, A. Yaser, and Z. Al-Khafaji, "AN ANSYS SIMULATION STUDY ON THE EFFECT OF APPLYING TITA-NIUM ALLOY (TI-6AL-4V) COATING FOR WIND TURBINE GEAR," *Academic Journal of Manufacturing Engineering*, vol. 22, no. 4, 2024.

[29] N. S. Radhi, H. H. Jamal Al-deen, R. Safaa Hadi, N. Al-Ghaban, and Z. S. Al-Khafaji, "Preparation And Investigation A Hydroxyapatite Layer Coating On Titanium Substrate For Surgical Implants.," *Journal of Nanostructures*, 2022.

[30] N. D. Fahad, N. S. Radhi, Z. S. Al-Khafaji, and A. A. Diwan, "Surface modification of hybrid composite multilayers spin cold spraying for biomedical duplex stainless steel," *Heliyon*, 2023, doi: 10.1016/j.heliyon.2023.e14103.

[31] S. Sattar, Y. Alaiwi, N. S. Radhi, and Z. Al-khafaji, "Numerical Simulation for Effect of Composite Coating (TiO2 + SiO2) Thickness on Steam Turbine Blades Thermal and Stress Distribution," *ACADEMIC JOURNAL OF MANUFACTURING ENGINEERING*, vol. 21, no. 4, 2023.

[32] I. P. Torres-Avila *et al.*, "Surface modification of the Ti-6Al-4V alloy by anodic oxidation and its effect on osteoarticular cell proliferation," *Coatings*, vol. 10, no. 5, p. 491, 2020.

[33] F. P. Lestari, Y. R. Sari, F. Rokhmanto, T. Asmaria, and A. W. Pramono, "Surface Modification of Ti-6Al-4V Alloy By Anodization Technique at Low Potential to Produce Oxide Layer," *Journal of Electronics, Electromedical Engineering, and Medical Informatics*, vol. 2, no. 3, pp. 93–102, 2020.

[34] A. Ossowska, A. Zieliński, J.-M. Olive, A. Wojtowicz, and P. Szweda, "Influence of Two-Stage Anodization on Properties of the Oxide Coatings on the Ti–13Nb–13Zr Alloy," *Coatings*, vol. 10, no. 8, p. 707, 2020.

[35] A. N. Najim, M. T. Mohammed, and M. A. Albozahid, "Morphology, Topography and Wettability of CP-Ti after Anodization Process for Biomedical Applications," in *Journal of Physics: Conference Series*, IOP Publishing, 2021, p. 12006.

[36] A. Stróż *et al.*, "Biological Activity and Thrombogenic Properties of Oxide Nanotubes on the Ti-13Nb-13Zr Biomedical Alloy," *Journal of Functional Biomaterials*, vol. 14, no. 7, p. 375, 2023.

[37] J. Jakubowicz, G. Adamek, and L. Smardz, "Porous surface state analysis of anodized titanium for biomedical applications," *Metallurgical and Materials Transactions A*, vol. 53, pp. 86–94, 2022.

[38] T. Li, D. Ding, and N. Li, "Anodic fabrication of Ti-Ni-Si-O nanostructures on Ti10Ni5Si alloy," *Materials*, vol. 12, no. 8, p. 1315, 2019.

[39] L. Zaraska *et al.*, "Influence of anodizing conditions on generation of internal cracks in anodic porous tin oxide films grown in NaOH electrolyte," *Applied Surface Science*, vol. 439, pp. 672–680, 2018.

[40] F. Likibi, M. Assad, C. Coillard, G. Chabot, and C. H. Rivard, "Bone integration and apposition of porous and non porous metallic orthopaedic biomaterials," in *Annales de chirurgie*, 2005, pp. 235–241.

[41] R. Lu *et al.*, "Effects of hydrogenated TiO2 nanotube arrays on protein adsorption and compatibility with osteoblast-like cells," *International Journal of Nanomedicine*, pp. 2037–2049, 2018.

[42] S. Minagar, Y. Li, C. C. Berndt, and C. Wen, "Cell response and bioactivity of titania–zirconia–zirconium titanate nanotubes with different nanoscale topographies fabricated in a non-aqueous electrolyte," *Biomaterials science*, vol. 3, no. 4, pp. 636–644, 2015.

[43] Z. M. Abed Janabi, H. S. Jaber Alsalami, Z. S. Al-Khafaji, and S. A. Hussien, "Increasing of the corrosion resistance by preparing the trivalent nickel complex," *Egyptian Journal of Chemistry*, 2021, doi: 10.21608/EJCHEM.2021.100733.4683.

[44] N. S. RADHI, Z. AL-KHAFAJI, B. M. MAREAI, S. RADHI, and A. M. ALSAEGH, "REDUCING OIL PIPES CORROSION BY (ZN-NI) ALLOY COATING ON LOW CARBON STEEL SUBSTRATE BY SUSTAINABLE PROCESS," *Journal of Engineering Science and Technology*, vol. 18, no. 3, pp. 1624–1638, 2023.

[45] S. Sreekantan, Z. Lockman, R. Hazan, M. Tasbihi, L. K. Tong, and A. R. Mohamed, "Influence of electrolyte pH on TiO2 nanotube formation by Ti anodization," *Journal of Alloys and Compounds*, vol. 485, no. 1–2, pp. 478–483, 2009.